


Direct time-of-flight distributed analysis of nonlinear forward scattering: supplement

KAVITA SHARMA,¹ ELAD ZEHAVID,¹ H. HAGAI DIAMANDI,¹ GIL BASHAN,¹ YOSEF LONDON,^{1,2} AND AVI ZADOK^{1,*} 

¹ Faculty of Engineering and Institute for Nano-Technology and Advanced Materials, Bar-Ilan University, Ramat-Gan 5290002, Israel

² Current address: Applied Physics Division, Soreq NRC, Yavne 81800, Israel

*Corresponding author: Avinoam.Zadok@biu.ac.il

This supplement published with Optica Publishing Group on 11 April 2022 by The Authors under the terms of the [Creative Commons Attribution 4.0 License](https://creativecommons.org/licenses/by/4.0/) in the format provided by the authors and unedited. Further distribution of this work must maintain attribution to the author(s) and the published article's title, journal citation, and DOI.

Supplement DOI: <https://doi.org/10.6084/m9.figshare.19400921>

Parent Article DOI: <https://doi.org/10.1364/OPTICA.450810>

Supplementary Information: Direct time-of-flight distributed analysis of nonlinear forward scattering

Kavita Sharma¹, Elad Zehavi¹, H. Hagai Diamandi¹, Gil Bashan¹, Yosef London^{1,2}, and Avi Zadok^{1,*}

¹Faculty of Engineering and Institute for Nano-Technology and Advanced Materials, Bar-Ilan University, Ramat-Gan 5290002, Israel

²Currently with Applied Physics Division, Soreq NRC, Yavne 81800, Israel

*Corresponding Author: Avinoam.Zadok@biu.ac.il

1. Inter-modal forward stimulated Brillouin scattering in polarization maintaining fibers

Inter-modal forward stimulated Brillouin scattering (forward SBS) in polarization maintaining (PM) fibers has been described at length in a recent reference [1]. The process is presented briefly here for completeness and the convenience of the reader. Figure 1(a) shows a schematic cross-section of a panda-type, PM fiber, with a thin coating layer. The cladding cross-section includes two strain rods of silica doped with B₂O₃ glass. Expansion of the rods during fiber production induces permanent strain and birefringence between the slow \hat{x} axis and fast \hat{y} axis (see Fig. 1(a)). We denote the effective indices of the optical modes in the \hat{x} and \hat{y} polarizations as $n_{s,f}$, respectively, and the difference between the two as Δn . The value of Δn in panda-type PM fibers is of the order of $2\text{-}6 \times 10^{-4}$ refractive index units (RIU) [2].

The PM fiber cross section supports a large number of guided acoustic modes, which propagate in the axial direction \hat{z} [1]. We denote the normalized transverse profiles of material displacement in mode m as $\vec{u}_m(x,y)$ [m⁻¹], where x,y are the transverse coordinates in the \hat{x} and \hat{y} directions, respectively, and m is a positive integer. The profiles are normalized so that $(1/\rho_1) \iint \rho(x,y) |\vec{u}_m(x,y)|^2 dx dy = 1$. Here $\rho(x,y)$ denotes the local equilibrium density, and ρ_1 is the density of silica. The transverse profiles span the entire cross-section of the cladding and may also reach into thin coating layers [3,4]. Each mode is characterized by a cut-off frequency Ω_m , below which it may not propagate in the axial direction. The cut-off frequencies of modes relevant to this work are on the order of 100 MHz. Due to the lack of radial symmetry in the PM fiber cross-section, the displacement profiles $\vec{u}_m(x,y)$ are generally more complex than those of corresponding modes in standard, single-mode fibers [5,6]. For example, Fig. 1(b) shows the normalized transverse profile of the density oscillations magnitude $\nabla \cdot \vec{u}_m(x,y)/\rho(x,y)$, for one guided acoustic mode, with a cut-off frequency of 126 MHz.

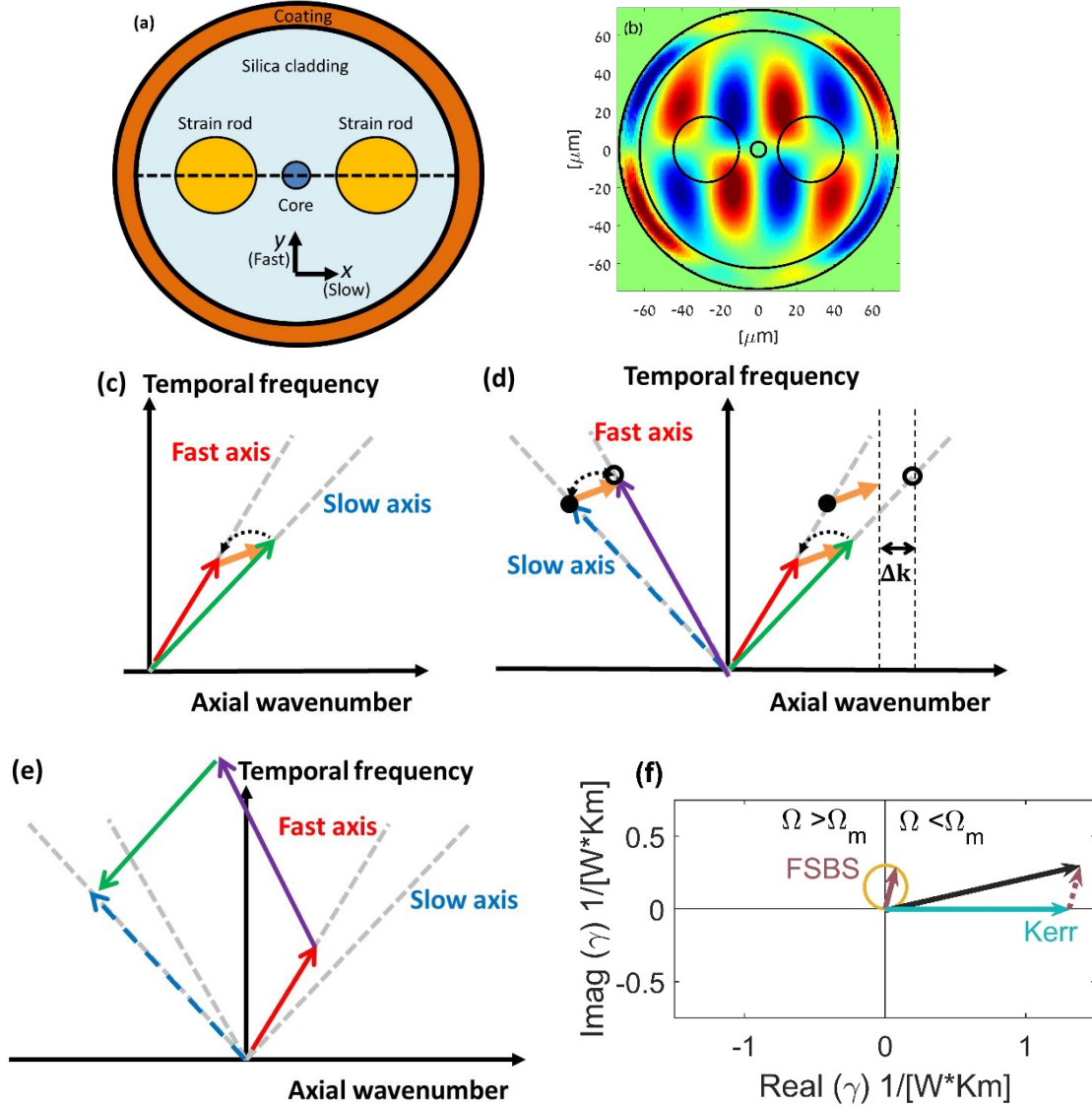
Consider two continuous optical pump tones of optical frequencies $\omega_p \pm \frac{1}{2}\Omega$, that co-propagate in the positive \hat{z} direction along a PM fiber. Here ω_p is a central optical frequency and Ω represents a radio-frequency offset. The higher-frequency pump tone is polarized along the slow principal axis \hat{x} , whereas the lower-frequency one is aligned with the fast axis \hat{y} . We denote the complex magnitudes of the two waves (in Volts) as $A_{1,2}$, respectively. The two pump tones induce an electro-strictive driving force per unit volume, given by [1,7]:

$$\vec{F}(r,\phi,z,t) = \frac{1}{4nc} \vec{f}(r,\phi) \tilde{P}(\Omega) \exp(jKz - j\Omega t) + c.c. \quad (1)$$

Here z denotes the axial coordinate, t stands for time, r and ϕ are the radial and azimuthal transverse coordinates, respectively, c is the speed of light in vacuum, and $n \approx n_{s,f}$. Also, in Eq. (1) $\tilde{P}(\Omega) = 2n\epsilon_0 c A_1 A_2^*$ [W] with ϵ_0 denoting the vacuum permittivity, and $K = \Delta n \omega_p / c + n \Omega / c \approx \Delta n \omega_p / c$ is the axial wavenumber of the electro-strictive driving force. Finally, the transverse profile $\vec{f}(r,\phi)$ of the driving force equals [1,7]:

$$\vec{f}(r, \phi) = 2a_1 \frac{\partial E_T(r)}{\partial r} E_T(r) [\sin(2\phi)\hat{r} + \cos(2\phi)\hat{\phi}]. \quad (2)$$

In Eq. (2), \hat{r} and $\hat{\phi}$ represent the unit vectors in the radial and azimuthal directions, respectively, and $E_T(r)$ [m⁻¹] is the normalized transverse profile of the optical mode which is assumed to be the same for both principal axes. The optical mode profile is normalized to $2\pi \int |E_T(r)|^2 r dr = 1$. The coefficient a_1 is drawn from elements of the photo-elastic tensor \mathbf{p} of silica: $a_1 = -n^4(p_{11} - p_{12}) = 0.66$ [5,7].



Supplementary Figure 1. (a): Schematic cross-section of a panda-type, PM fiber with a thin coating layer. (b): Calculated normalized transverse profile of the density oscillations magnitude for one guided acoustic mode of a coated PM fiber, with a cut-off frequency of 126 MHz. (c): Schematic illustration of frequency and wavenumber conservation in inter-modal forward SBS in a PM fiber. (d): Schematic illustration of photo-elastic cross-polarization switching of an optical probe wave, due to guided acoustic waves that are stimulated in inter-modal forward SBS. The scattering of the probe wave is non-reciprocal: It may take place for probe waves of specific optical frequencies that counter-propagate with respect to the inter-modal forward SBS pumps. Probe waves of the same frequencies that co-propagate with the pumps are unaffected due to wavenumbers mismatch. (e): Schematic illustration of cross-polarization switching of a probe wave through Kerr four-wave mixing with the two forward SBS pump waves. The process adds up with the contribution of photo-elastic scattering. (f): Phasor addition of nonlinear coefficients of inter-modal Kerr effect four-wave mixing and forward SBS [8].

The electro-strictive driving force may stimulate the oscillations of guided acoustic modes of the PM fiber. Effective stimulation requires that the acoustic mode should match the frequency Ω and axial wavenumber K of the driving force [1,5,7]. This condition can be met close to the modal cut-off, $\Omega \approx \Omega_m$ [1,5,7] (see Fig. 1(c)). The axial wavenumber K is of the order of $1,000 \text{ rad} \times \text{m}^{-1}$. This value is 2-3 orders of magnitude larger than the axial acoustic wavenumbers in intra-modal forward SBS, such as in standard single-mode fibers [5,6]. Nevertheless, K remains much smaller than the wavenumbers of bulk acoustic waves of the same frequency Ω in the silica cladding or the strain rods [1]. Therefore, the acoustic waves involved in inter-modal forward SBS are almost entirely transverse. The material displacement \vec{u}_m is largely confined to the transverse plane as well.

The displacement (in meters) of acoustic mode m stimulated by the electro-strictive driving force per unit volume \vec{F} can be expressed as:

$$\vec{U}_m(x,y,z,t) = B_m(\Omega) \vec{u}_m(x,y) \exp(jKz - j\Omega t) + c.c., \quad (3)$$

with a modal magnitude $B_m(\Omega) [\text{m}^2]$ that is given by:

$$B_m(\Omega) = \frac{1}{4nc\rho_1} \frac{\iint \vec{u}_m^\dagger(x,y) \cdot \vec{f}(x,y) dx dy}{\Omega_m^2 - \Omega^2 - j\Gamma_m \Omega} \tilde{P}(\Omega) = \frac{1}{4nc\rho_1} Q_{ES}^{(m)} H_m(\Omega) \tilde{P}(\Omega) \quad (4)$$

The modal magnitude depends on frequency according to $H_m(\Omega) \equiv 1/(\Omega_m^2 - \Omega^2 - j\Gamma_m \Omega)$. It is maximal at the modal cut-off frequency, $\Omega = \Omega_m$. Γ_m denotes the modal linewidth, which also signifies the decay rate of acoustic energy. The linewidth is determined by dissipation in silica, strain rods and coating, and also by the transmission of acoustic energy towards surrounding media. This latter dependence forms the basis of forward SBS sensors of coatings and liquids outside the fiber cladding, where light cannot reach [9]. The displacement magnitude of the stimulated acoustic mode scales with the overlap integral $Q_{ES}^{(m)} \equiv \iint \vec{u}_m^\dagger(x,y) \cdot \vec{f}(x,y) dx dy$ between the transverse profiles of modal displacement and driving force [1,5,7].

The material displacement of the stimulated acoustic modes is associated with strain in the fiber. Strain, in turn, gives rise to perturbations of the dielectric tensor elements, through the mechanism of photo-elasticity [5,7]. Since the optical fields as well as the acoustic displacements are almost entirely transverse, the analysis may be restricted to a 2×2 dielectric perturbations tensor in the transverse plane only. For the purpose of this study, the off-diagonal term of the dielectric perturbations tensor is the most relevant:

$$\delta\epsilon_{m,xy}(x,y,z,t) = B_m(\Omega) \mu_{m,xy}(x,y) \exp(jKz - j\Omega t) + c.c., \quad (5)$$

where:

$$\mu_{m,xy}(x,y) = -n^4 p_{44} \left(\frac{\partial u_{m,x}}{\partial y} + \frac{\partial u_{m,y}}{\partial x} \right). \quad (6)$$

In Eq. (6), p_{44} is an element of the photo-elastic tensor \mathbf{p} of silica, $-n^4 p_{44} = a_1/2$ (0.33 in silica), and $u_{m,x}$, $u_{m,y}$ are the \hat{x} and \hat{y} components of the normalized displacement profile of the acoustic mode \vec{u}_m , respectively. The effect of the acoustic mode on the propagation of optical waves scales with the spatial overlap integral between the transverse profiles of perturbations to the dielectric tensor element and the optical mode:

$$\begin{aligned} \overline{\delta\epsilon}_{m,xy}(z,t) &= B_m(\Omega) \left[\iint \mu_{m,xy}(x,y) |E_T(x,y)|^2 dx dy \right] \exp(jKz - j\Omega t) + c.c. \\ &= B_m(\Omega) Q_{PE}^{(m)} \exp(jKz - j\Omega t) + c.c. \end{aligned} \quad (7)$$

Here we have defined the overlap integral: $Q_{PE}^{(m)} \equiv \iint \mu_{m,xy}(x,y) |E_T(x,y)|^2 dx dy [\text{m}^2]$.

The photo-elastic perturbations couple optical power between the two pump tones. Let us denote the power of the pump waves of frequencies $\omega_p \pm \frac{1}{2}\Omega$ as $P_{1,2}(z) = 2n\epsilon_0 c |A_{1,2}(z)|^2$ [W]. Neglecting linear losses over the comparatively short fiber lengths of interest, the power levels change along the fiber according to [1]:

$$\frac{dP_1(z)}{dz} = -2\text{Im}\left\{\sum_m \gamma_m(\Omega)\right\}P_1(z)P_2(z), \quad (8)$$

$$\frac{dP_2(z)}{dz} = +2\text{Im}\left\{\sum_m \gamma_m(\Omega)\right\}P_1(z)P_2(z). \quad (9)$$

In Eq. (8) and Eq. (9) we have defined the opto-mechanical nonlinear coefficient of forward SBS $\gamma_m(\Omega)$, in units of $\text{W}^{-1}\text{m}^{-1}$:

$$\gamma_m(\Omega) = \frac{k_p Q_{ES}^{(m)} Q_{PE}^{(m)}}{8n^2 c \rho_1} H_m(\Omega) = \frac{k_p Q_{ES}^{(m)} Q_{PE}^{(m)}}{8n^2 c \rho_1} \frac{1}{\Omega_m^2 - \Omega^2 - j\Gamma_m \Omega}. \quad (10)$$

Here k_p is the vacuum wavenumber at the optical frequency ω_p . The forward SBS coefficient assumes its largest magnitude at the cut-off frequency:

$$\gamma_{0m} \equiv \gamma_m(\Omega_m) = j \frac{k_p Q_{ES}^{(m)} Q_{PE}^{(m)}}{8n^2 c \rho_1 \Gamma_m \Omega_m}. \quad (11)$$

Since the imaginary part of the forward SBS coefficient is positive, Eq. (8) and Eq. (9) suggest that the higher-frequency optical pump wave is attenuated in the process, whereas the lower-frequency one is amplified. The modal linewidths Γ_m are typically of the order of few MHz, at most. We may therefore approximate $\Omega \approx \Omega_m$ within the modal linewidths, leading to:

$$\gamma_m(\Omega) \approx \gamma_{0m} \frac{1}{1 + 2j(\Omega_m - \Omega)/\Gamma_m}. \quad (12)$$

In addition to the coupling of power between the two pump tones, the acoustic waves generated in the inter-modal forward SBS process may also scatter an optical probe wave from one principal axis to the other [1] (see Fig. 1(d)). Cross-polarization switching via forward SBS adds up with similar scattering via the Kerr effect [8] (Fig. 1(e)). Both contributions are the most efficient for a specific offset in optical frequencies between pumps and probe [1]:

$$\Delta\omega_{opt} = \frac{2n}{\Delta n} \Omega. \quad (13)$$

The optimal offset $\Delta\omega_{opt}$ is simply proportional to the detuning Ω between the two pump tones. In panda-type PM fibers, the optimal frequency difference is on the order of THz [1]. Note that $\Delta\omega_{opt}$ may vary with fiber position due to residual fluctuations in the PM fiber birefringence Δn . Polarization switching of probe light is non-reciprocal: Probe waves that counter-propagate with respect to the pump tones may be partially scattered to the orthogonal polarization, whereas co-propagating probe waves of the same frequencies are unaffected due to wavenumbers mismatch [1] (see Fig. 1(d)).

Let us consider an optical probe wave of frequency ω_{sig} that is polarized along the fast $\hat{\mathbf{y}}$ axis and propagates in the $-\hat{\mathbf{z}}$ direction. We denote the magnitude of the probe wave as $A_{sig,y}$. The probe is partially coupled to a new field component $A_{sig,x}$ of $\hat{\mathbf{x}}$ polarization and optical frequency $\omega_{sig} - \Omega$, which also propagates in the $-\hat{\mathbf{z}}$ direction. The cross-polarization coupling is typically weak, and we may assume that $A_{sig,y}$ remains nearly constant and that $|A_{sig,y}| \gg |A_{sig,x}|$ at all fiber positions. At that condition, we obtain:

$$-\frac{dA_{sig,x}(z,\Omega)}{dz} = j \left[\sum_m \gamma_m(\Omega) + \gamma_{Kerr} \right] \tilde{P}(\Omega) A_{sig,y} \exp(j\Delta k \cdot z). \quad (14)$$

The negative sign on the left-hand side represents propagation of the probe wave in the negative $-\hat{z}$ direction. In Eq. (14), γ_{Kerr} [$\text{W}^{-1}\text{m}^{-1}$] is the nonlinear coefficient that quantifies the Kerr effect. Note that unlike the forward SBS coefficient, γ_{Kerr} is purely real and does not depend on the difference Ω between the optical pump frequencies. The magnitude of the overall effective nonlinear coefficient, $\gamma_{eff}(\Omega) \equiv \sum_m \gamma_m(\Omega) + \gamma_{Kerr}$, is determined by phasor addition of the forward SBS and Kerr effect contributions [8] (Fig. 1(f)). Also in Eq. (14), the wavenumber mismatch term Δk is defined as [1]:

$$\Delta k = \Delta n(\omega_{sig} - \omega_p - \Delta\omega_{opt})/c. \quad (15)$$

Polarization switching of the probe wave is wavenumber matched when the difference in optical frequencies $(\omega_{sig} - \omega_p)$ between pumps and probe equals the optimal value $\Delta\omega_{opt}$ of Eq. (13) [1]. Following propagation along a uniform fiber section of length Δz , the magnitude of the scattered probe wave component is given by:

$$A_{sig,x}(\Delta z, \Omega) = -j\gamma_{eff}(\Omega) \tilde{P}(\Omega) \cdot \text{sinc}\left(\frac{\Delta k \cdot \Delta z}{2}\right) \exp\left(j \frac{\Delta k \cdot \Delta z}{2}\right) A_{sig,y} \Delta z. \quad (16)$$

The cross-polarization switching of the probe wave varies with its optical frequency according to birefringence-related wavenumber matching considerations, and with the offset Ω between the two pump tones according to the inter-modal forward SBS spectrum. The above dependence on Δz is strictly valid only for continuous-wave pump tones. When pump pulses are used, the finite lifetime of acoustic waves stimulation leads to differences between the contributions of Kerr effect and photo-elastic scattering (see greater detail in Supplementary Information 3 below). The exact spectrum of the probe wave scattering becomes time-variant. However, the decrease in scattering strength with $|\Delta k|$ remains.

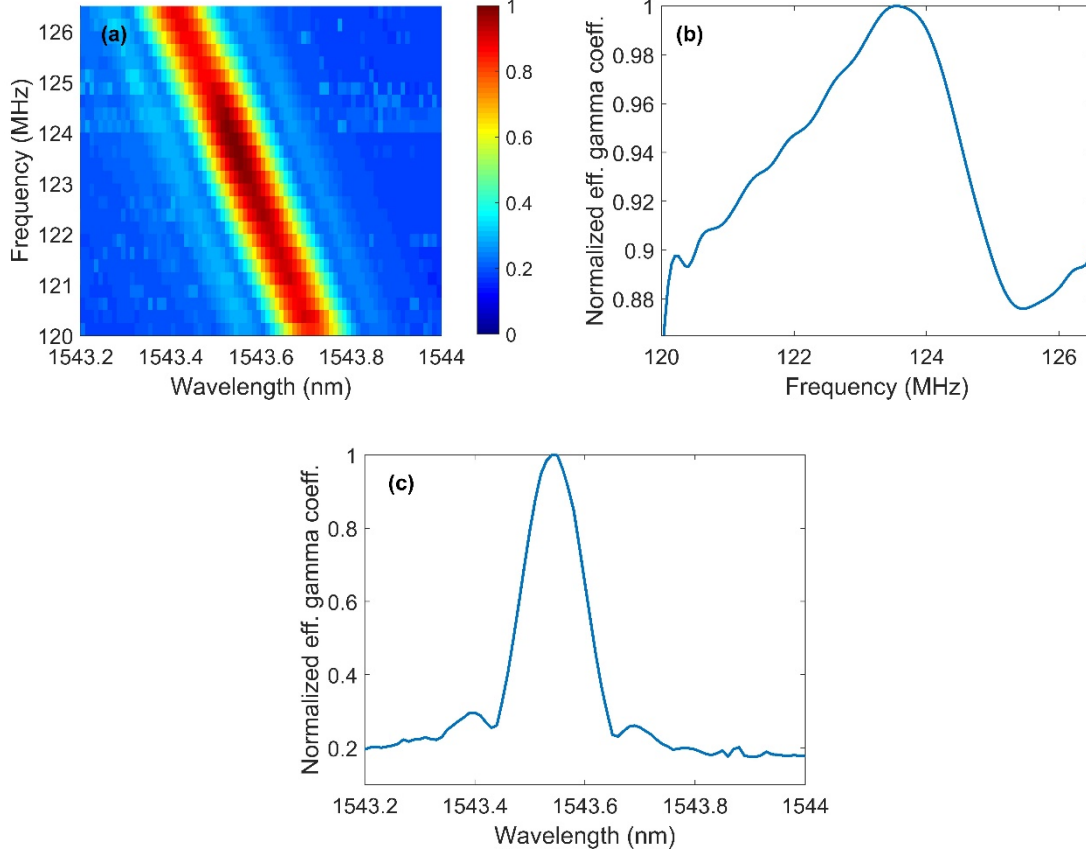
The nonlinear coefficient $\gamma_{eff}(\Omega)$ may be retrieved through measurements of $A_{sig,x}$ at $z = 0$, the input end of the two pump tones and the output end of the probe wave. When a pulsed amplitude envelope is overlaid on top of the two pump tones, the measurement of $A_{sig,x}$ following a delay of τ seconds may be related to the local $\gamma_{eff}(\Omega)$ at a position $z = \frac{1}{2}v_g\tau$. Here v_g denotes the group velocity of light in the fiber. The spatial resolution of the analysis is given by $\Delta z = \frac{1}{2}v_g\Delta\tau$, where $\Delta\tau$ is the pulse duration.

2. Nonlinear polarization switching of an optical probe wave as a function of its wavelength and the frequency difference between the two pump waves.

Figure 2(a) presents a two-dimensional scan of the normalized cross-polarization switching of the probe wave as a function of both its wavelength λ_{sig} and the difference Ω between the optical frequencies of the two pump waves. Measurements were taken on a 60 meters long section of PM fiber coated with polyimide. The central wavelength of the two pump waves was 1550 nm. (For details of the measurement setup, see Main Text). The intensity of the pump tones was modulated by 600 ns long pulses. Data was collected when the pumps pulse was in complete overlap with the section of fiber under test (see Supplementary Information 3 below). Inter-modal forward SBS in that section has a resonance frequency at 123 MHz (see Main Text). The difference between the probe wavelength of maximum polarization switching and that of the pumps increases with Ω , as predicted by Eq. (13) above.

Figure 2(b) shows the measured normalized nonlinear coefficient $\gamma_{eff}(\Omega)$. For each frequency Ω , the reading at the probe wavelength λ_{sig} of maximum scattering was used. A baseline of probe wave polarization switching is observed for all values of Ω , due to Kerr effect four-wave mixing. The additional contribution of photoelastic scattering due to stimulated acoustic waves is observed near 124 MHz. The phasor addition of the two contributions manifests in a maximum spectral slope at the frequency

of the inter-modal forward SBS resonance. Figure 2(c) shows the normalized magnitude of the probe wave scattering as a function of λ_{sig} , for $\Omega = 2\pi \times 123.5$ MHz. Maximum scattering is observed at a probe wavelength of 1543.5 nm. The scattering magnitude follows a sinc squared dependence on the detuning of the probe wavelength from its optimum value, as suggested by Eq. (16).

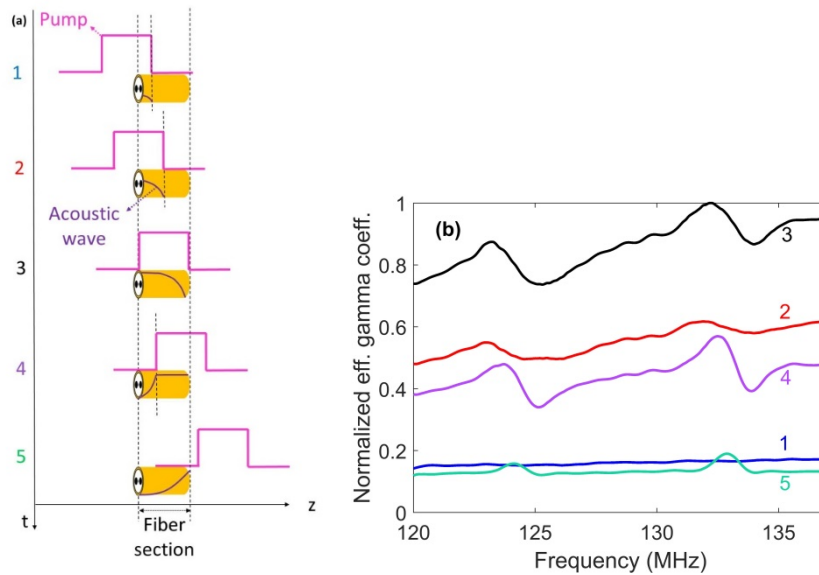


Supplementary Figure 2. (a): Measured normalized magnitude of an optical probe wave that is nonlinearly scattered from the fast axis to the slow axis of a PM fiber, as a function of its wavelength and the difference in frequencies Ω between two pump tones. A 60 meters-long section of fiber coated with polyimide was used. The pump waves propagated in the positive \hat{z} direction, whereas the probe wave was launched from the opposite end and propagated in the $-\hat{z}$ direction. The mean wavelength of the pump waves was 1550 nm. The duration of the pumps pulse was 600 ns. Data was sampled when the pumps pulse was in complete overlap with the section under test (see Section 3 below). The difference between the probe wavelength of maximum switching and that of the pumps scales with Ω , as anticipated. (b): Measured normalized nonlinear coefficient γ_{eff} as a function of frequency Ω . For each frequency, data at the probe wavelength of maximum polarization switching was used. Nonlinear scattering of the probe wave is observed at all values of Ω due to Kerr effect four-wave mixing. Additional contribution due to photoelastic scattering by stimulated acoustic waves is obtained near 124 MHz. The phasor addition of the two contributions manifests in a maximum spectral slope at the frequency of the inter-modal forward SBS resonance. (c): Measured normalized magnitude of the nonlinear probe wave scattering as a function of wavelength, with Ω set to $2\pi \times 123.5$ MHz. Scattering is the strongest at a wavelength of 1543.55 nm and follows a sinc squared dependence on detuning from this optimum value as suggested by Eq. (16).

3. Interplay of probe wave scattering contributions due to Kerr effect four-wave mixing and stimulated acoustic waves.

Figure 3(a) illustrates the build-up of stimulated acoustic waves along a fiber section, at several instances following the arrival of two pulsed pump tones. Figure 3b presents corresponding measurements of nonlinear scattering spectra of a counter-propagating probe wave. Measurements were taken over a 60 meters-long section of PM fiber coated with polyimide, using 600 ns-long pulses. As

the leading edge of the pumps pulse reaches the section under test (noted as (1) in both panels), scattering of the probe wave is dominated by the Kerr effect. Scattering is therefore independent of the frequency difference Ω between the two pump waves. Following 300 ns (instance (2) in panel (a) and trace (2) in panel (b)), the inter-modal Brillouin stimulation of guided acoustic modes near 123 MHz and 133 MHz frequencies becomes appreciable, and photo-elastic contributions appear in the probe scattering spectrum.



Supplementary Figure 3. (a): Illustrations of pulsed envelope of two pump tones along a section of fiber under test, and of the normalized magnitude of acoustic waves generated in an inter-modal forward SBS process. Five instances are shown: (1) immediately upon arrival of the pumps pulse; (2) during the build-up of the stimulated acoustic waves; (3) when the acoustic waves magnitude approaches its potential steady-state value; (4) as the pumps pulse is leaving the section under test and the acoustic waves begin to decay; and (5) towards the end of the acoustic waves decay. (b): Measured normalized magnitude of probe wave nonlinear switching as a function of the frequency difference Ω between the two pump tones, in a 60 meters long section of PM fiber coated with polyimide. The duration of pumps pulses was 600 ns. The five traces show data taken at different times delays following the arrival of the leading edge of pulsed pump tones: 100, 300, 600, 800 and 1300 ns. The five delays correspond to the different stages of the process illustrated in panel (a). Scattering of the probe wave due to Kerr effect four-wave mixing is instantaneous: it increases with time as the leading edge of the pulsed pumps fills the length of fiber under test and decreases as the trailing edge leaves that section (trace (1)). The contribution due to forward SBS builds up and decays more slowly due to acoustic modal lifetimes. The phasor addition of the Kerr effect and photo-elastic contributions manifests in a maximum spectral slope at the frequencies of inter-modal forward SBS resonance (traces (2) through (4)). Towards the end of the process (trace (5)), contributions of photo-elastic scattering alone appear as spectral peaks at the same frequencies.

The build-up of the acoustic waves manifests in a maximum spectral slope in the probe wave scattering near the two resonance frequencies, due to the interplay of Kerr and photo-elastic contributions. In addition, the baseline of scattering magnitude increases, as the pumps pulse is filling the entire length of the fiber section under test. The scattering magnitude reaches a maximum following 600 ns (3), when the Brillouin stimulation of acoustic waves approaches its steady-state magnitude. When the pumps pulse begins to leave the fiber section (time stamp (4), following 800 ns), the Kerr effect contribution drops accordingly while the stimulated acoustic waves decay more slowly according to their lifetimes.

Finally, the Kerr baseline vanished completely when the pumps pulse had left the fiber entirely ((5), 1300 ns). The scattering of the probe wave due to stimulated acoustic waves persists for additional hundreds of ns. Note that the scattering spectrum at this stage takes up the peaks shape that is characteristic of SBS alone. Peaks in trace (5) appear at the same frequencies where maximal spectral slopes are observed in traces (2) through (4). The continued oscillations of stimulated acoustic waves

after the pumps pulse had ended lead to non-local artifacts in the distributed analysis of forward scattering and restrict its spatial resolution to the order of tens of meters. This limitation does not affect the analysis of Kerr forward scattering alone, when Ω is detuned from forward SBS resonances.

Supplementary References

- [1] G. Bashan, H. H. Diamandi, Y. London, K. Sharma, K. Shemer, E. Zehavi, and A. Zadok, “Forward stimulated Brillouin scattering and opto-mechanical non-reciprocity in standard polarization maintaining fibres,” *Light Sci. Appl.* **10**, 119 (2021).
- [2] R. Guan, F. Zhu, Z. Gan, D. Huang, and S. Liu, “Stress birefringence analysis of polarization maintaining optical fibres,” *Opt. Fiber Technol.* **11**, 240-254 (2005).
- [3] D. M. Chow, and L. Thévenaz, “Forward Brillouin scattering acoustic impedance sensor using thin polyimide-coated fiber,” *Opt. Lett.* **43**, 5467-5470 (2018).
- [4] H. H. Diamandi, Y. London, G. Bashan, and A. Zadok, “Distributed opto-mechanical analysis of liquids outside standard fibers coated with polyimide,” *Appl. Phys. Lett. – Photon.* **4**, 016105 (2019).
- [5] R. M. Shelby, M. D. Levenson, and P. W. Bayer, “Guided acoustic-wave Brillouin scattering,” *Phys. Rev. B* **31**, 5244–5252 (1985).
- [6] A. S. Biryukov, M. E. Sukharev, and E. M. Dianov, “Excitation of sound waves upon propagation of laser pulses in optical fibers,” *J. Quant. Elect.* **32**, 765-775 (2002).
- [7] M. S. Kang, A. Brenn, and P. St. J. Russell, “All-optical control of gigahertz acoustic resonances by forward stimulated interpolarization scattering in a photonic crystal fiber,” *Phys. Rev. Lett.* **105**, 153901 (2010).
- [8] Y. London, H. H. Diamandi, G. Bahsan, and A. Zadok, “Distributed analysis of nonlinear wave mixing in fiber due to forward Brillouin scattering and Kerr effects,” *Appl. Phys. Lett. – Photon.* **3**, 110804 (2018).
- [9] Y. Antman, A. Clain, Y. London, and A. Zadok, “Optomechanical sensing of liquids outside standard fibers using forward stimulated Brillouin scattering,” *Optica* **3**, 510-516 (2016).